The Active Site Cysteine of Arginine Kinase: Structural and Functional Analysis of Partially Active Mutants[†,‡]

James L. Gattis,[§,||] Eliza Ruben,[||] Marcia O. Fenley,[||] W. Ross Ellington,[||,⊥] and Michael S. Chapman*[,§,||]

Departments of Chemistry and Biochemistry and of Biological Science and Institute of Molecular Biophysics, Florida State University, Tallahassee, Florida 32306-4380

Received January 29, 2004; Revised Manuscript Received May 3, 2004

ABSTRACT: Arginine kinase buffers cellular ATP levels by catalyzing reversible phosphoryl transfer between ATP and arginine. A conserved cysteine has long been thought important in catalysis. Here, cysteine 271 of horseshoe crab arginine kinase has been mutated to serine, alanine, asparagine, or aspartate. Catalytic turnover rates were 0.02−1.0% of wild type, but the activity of uncharged mutations could be partially rescued with chloride. Steady-state binding constants were slightly increased, more so for phospho-L-arginine than ADP. Substrate binding synergy observed in many phosphagen kinases was reduced or eliminated in mutant enzymes. The crystallographic structure of the alanine mutant at 2.3 Å resolution, determined as a transition state analogue complex with arginine, nitrate, and MgADP, was nearly identical to wild type. Enzyme−substrate interactions are maintained as in wild type, and substrates remain at least roughly aligned for in-line phosphoryl transfer. Homology models with serine, asparagine, or aspartate replacing the active site cysteine similarly show only minor structural changes. Most striking, however, is the presence in the C271A mutant crystallographic structure of a chloride ion within 3.5 Å of the nonreactive N_η substrate nitrogen, approximating the position of the sulfur in the wild-type's cysteine. Together, the results contradict prevailing speculation that the cysteine mediates a substrate-induced conformational change, confirm that it is the thiolate form that is relevant to catalysis, and suggest that one of its roles is to help to enhance the catalytic rate through electrostatic stabilization of the transition state.

Phosphagen kinases play a central role in maintaining energy homeostasis by buffering cellular ATP concentrations. A variety of phosphagen kinases are found in nature; however, creatine kinase (CK)[1] found throughout the metazoa and arginine kinase (AK) distributed primarily in the invertebrates are the most thoroughly characterized (*1*, *2*). All phophagen kinases catalyze the reversible transfer of the terminal phosphate of ATP to the guanidinium group of an "energy storage" molecule. Specifically, arginine kinase catalyzes:

$$\text{MgATP} + \text{arginine} \leftrightarrow \text{MgADP} + \text{phospho-L-arginine} + \text{H}^+$$

Prior enzyme kinetic evaluations have shown that the arginine kinase reaction is consistent with a rapid equilibrium, random order substrate binding, bimolecular−bimolecular mechanism with phosphoryl transfer directly between substrates (*3*, *4*). The creatine kinase reaction is analogous with the exception of ordered substrate binding below a pH of 7 (*5*).

Phosphagen kinases contain a single reactive cysteine residue in each subunit located in a highly conserved peptide sequence common to all known phosphagen kinase sequences (*6*). X-ray crystallographic structures of transition state forms of AK (*7*) and CK (*8*) show analogous positions in the active site for this conserved residue. Early chemical modifications of the reactive cysteine with iodoacetamide identified a single cysteine residue per subunit in both AK and CK that was particularly sensitive to covalent modification (*6*, *9*). These initial experiments resulted in completely inactive enzymes, suggesting that the reactive cysteine was essential for catalysis. It has since been shown that covalent attachment of a small nonpolar ($-SCH_3$) group to the reactive cysteine of CK results in an enzyme with some residual catalytic activity (*10*). However, some have proposed that the residual activity remains from unmodified enzyme molecules (*11*).

Mutagenesis of the reactive cysteine residue of several creatine kinase isoforms has resulted in significant reduction of activity in chicken brain CK (CBCK; *12*), chicken cardiac

[†] Funded by National Institutes of Health Grant R01-GM55837 (M.S.C.) and the National Science Foundation through a research training grant (DBI96-02233; J.L.G.) and an ADVANCE fellowship (CHE-0137961; M.O.F.).

[‡] Coordinates and diffraction amplitudes have been deposited in the PDB with accession code 1SDO.

* To whom correspondence should be addressed. Tel: (850) 644-8354. Fax: (850) 644-7244. E-mail: chapman@sb.fsu.edu.

[§] Department of Chemistry and Biochemistry, Florida State University.

[||] Institute of Molecular Biophysics, Florida State University.

[⊥] Department of Biological Science, Florida State University.

[1] Abbreviations: AK, arginine kinase; ADP, adenosine diphosphate; ArgP, arginine phosphate; ATP, adenosine triphosphate; CK, creatine kinase; CBCK, chicken brain CK; HBCK, human brain CK; HMCK, human muscle CK; Mi_bCK, mitochondrial CK (basic sarcomeric isoform); DTT, dithiothreitol; EDTA, ethylenediaminetetraacetic acid; HEPES, *N*-(2-hydroxyethyl)piperazine-*N*′-2-ethanesulfonic acid.

10.1021/bi049793i CCC: $27.50
Published on Web 06/17/2004

mitochondrial CK (Mi_b-CK) (*13*), and human muscle CK (HMCK)(*14*) and complete loss of activity in the brain isoform of human CK (HBCK, *15*). However, the recovery of about half wild-type activity in a C278G mutant of chicken cardiac mitochondrial CK (Mi_b-CK), when measured at low pH, indicated that the cysteine might not be essential catalytically (*13*). Several mutations at this site lacked the substrate binding synergy characteristic of the wild-type enzyme (*13*). Residual activity and lost synergy following chemical modification of rabbit muscle CK or mutagenesis of Mi_b-CK were interpreted to indicate a role of the cysteine in substrate-induced conformational changes (*10*, *13*). However, until now, there has not been a structure of a cysteine-modified enzyme to help to elucidate the role.

Reactive cysteine mutations of Mi_b-CK that gave a neutrally charged side chain showed increased catalytic activity in the presence of chloride ions (*13*). This activation led to the proposal that the reactive cysteine of CK functions as a thiolate ion ($AA-CH_2-S^-$). Supporting evidence came from enzyme kinetic and spectroscopic titration experiments on wild-type and cysteine-substituted HMCK which showed that the pK_a of the reactive cysteine residue was between 5 and 6, about 2−3 pK_a units below its unperturbed value of 8.5 (*14*). At least in HMCK, the reactive cysteine is expected to be primarily deprotonated at neutral pH.

Recent crystal structures of substrate-free as well as transition state forms of both arginine kinase and creatine kinase confirm overall similarities in subunit structure between the two enzymes (*7*, *8*, *16*, *17*). Each subunit of CK and AK can be divided into two structural domains, a smaller amino-terminal domain comprising residues 1−99 in AK and a larger carboxyl-terminal domain formed by residues 100−357. The active site is comprised of residues mostly from the large domain, but the small domain also contributes to phosphagen binding. Comparison of the substrate-free to the transition state structure of AK has shown that although the active site cysteine (C271) is located in the large domain, it moves during catalysis with residues of the small domain (*16*). Transition state structures of both AK (*18*) and CK (*8*) show that the active site cysteine is located on a flexible loop that interacts with the guanidinium of arginine or creatine. In arginine kinase and creatine kinase, sulfur atoms of the cysteine side chain are found approximately 3.3 Å from the nonreactive nitrogen, i.e., the nitrogen that does not form a covalent bond to the phosphorus of substrate arginine or creatine. Superimposition of transition state forms of creatine kinase and arginine kinase results in excellent alignment of the guanidinium atoms of substrates creatine or arginine and shows clear homology in the position of the cysteine side chain.

The present study probes the role of the active site cysteine through joint structural and kinetic analysis of mutants of arginine kinase. The kinetic effects of mutating the active site cysteine, which are similar to those in creatine kinase, can now be understood in terms of the experimental (X-ray) structure of the transition state analogue form of the C271A mutant. Mutants in which Cys_{271} was changed to serine, asparagine, and aspartate were expressed and characterized kinetically but were not as readily crystallized. The effects of these mutations are rationalized through models based on homology with known structures and using a combination of simulated annealing and energy minimization.

MATERIALS AND METHODS

Materials. Reagents were obtained from Sigma-Aldrich, Fisher Scientific, and Roche Molecular Biochemicals unless otherwise noted.

Primer Synthesis and Mutagenesis. Oligonucleotide primers were designed to incorporate the desired mutations and used to produce mutagenic DNA with the QuikChange mutagenesis kit (Stratagene, Inc.). Single amino acid substitutions were accomplished by one to three nucleotide replacements for each amino acid substitution. Mutant plasmid DNA was transfected into commercially produced BL21(DE3) *Escherichia coli* competent cells (Stratagene, Inc.).

Expression and Purification. Mutants C271S, C271A, C271N, C271D, C271G, C271T, C271M, and C271Y were expressed in BL21(DE3) *E. coli* and purified from insoluble inclusion bodies using published methods (*19*). The refolding procedure was changed for wild type and C271A. In contrast to the previously published refolding protocol involving sequential dialysis, wild type and C271A were refolded by addition of a small volume of concentrated, denatured protein in 6 M urea to a large volume of 10 mM Tris (pH 8.1), 1 mM EDTA, 2 mM DTT, and 10 mM KCl with no denaturing agents. The final protein concentration after dilution was between 0.1 and 0.2 mg/mL. Diluted arginine kinase was incubated at 4 °C overnight, concentrated, and additionally purified with size-exclusion and anion-exchange chromatography.

Crystallization of C271A. C271A was concentrated to 27 mg/mL and dialyzed against components of the transition state analogue complex (*7*). Crystals were obtained using the hanging drop vapor diffusion method. Reservoir solutions contained 100 mM $MgCl_2$ and 100 mM HEPES in 18% or 20% poly(ethylene glycol), molecular weight 6000. Hanging drops were formed by addition of 4 μL of reservoir solution to 4 μL of protein solution containing 27 mg/mL C271A arginine kinase, 100 mM $MgCl_2$, 100 mM HEPES, 50 mM nitrate, 4 mM ADP, 20 mM arginine, and 1 mM DTT. All solutions used for crystallization were at pH 7.5 and 4 °C. Crystals appeared between 2 and 4 weeks and grew to 0.1−1 mm in two dimensions and approximately 0.05 mm in the third dimension.

Enzyme Kinetics. Wild-type and mutant arginine kinase initial activity was measured as described previously (*20*). In the current study, reaction rates for each protein were determined in solutions containing either 1 or 60 mM chloride. Activity was measured over a period of 1−15 min, depending on the activity of a given sample, and rates were estimated only during a time period that produced a linear increase in absorbance with time. Initial velocity was measured on a two-dimensional grid of six concentrations of phosphoarginine by six of ADP. Steady-state parameters K_{ia}, K_M, and V_{max} were obtained by averaging results over three independent evaluations using protein from at least two separate preparations, except for C271N for which all kinetic runs came from a single preparation.

Enzyme Kinetic Data Analysis. Rate measurements from the 6 × 6 matrix were fitted by nonlinear least squares (using SigmaPlot) to the rate equation for the random order

sequential bi-bi reaction mechanism (eq 1) and used to

$$v = V_{max}[\text{phosphoarginine}][\text{ADP}]/\alpha(K_{ia(\text{phosphoarginine})}K_{ia(\text{ADP})} + K_{ia(\text{ADP})}[\text{phosphoarginine}] + K_{ia(\text{phosphoarginine})}[\text{ADP}] + [\text{phosphoarginine}][\text{ADP}]) \quad (1)$$

determine the kinetic parameters V_{max}, K_{ia}(phosphoarginine), K_{ia}(ADP), and α (*21*). $K_{ia(\text{phosphoarginine})}$ and $K_{ia(\text{ADP})}$ refer to dissociation of the binary enzyme−substrate complexes E·phosphoarginine and E·ADP, respectively. K_M, the kinetic dissociation constant for the Michaelis complex E·phosphoarginine·ADP for a given substrate, was determined from $K_M = \alpha(K_{ia})$. Parameters were determined separately for wild type and each mutant in solutions containing 1 and 60 mM chloride. Each was repeated in triplicate with errors of the average parameters estimated from the triplicate variation.

Structure Determination of C271A. Crystals of C271A were frozen in liquid nitrogen after brief soaking in mother liquor containing 30% glycerol. Crystallographic data for the initial structure determination were collected at 100 K using a rotating anode source and an Rigaku Raxis II imaging plate as described previously for wild type (*19*). This data set was replaced during refinement with a slightly improved one collected at the Advanced Photon Source (at Argonne National Laboratory) from two crystals. Due to the crystals' small size, radiation damage was limiting. The rotating anode data set was collected from a single crystal. A total of 180 frames of diffraction data were processed using the HKL suite of programs (*22*); then the later frames were culled to strike an appropriate compromise between completeness and quality. The wild-type arginine kinase transition state structure was used as a probe for cross-rotation and translation searches using the CNS program. The correct solution at 7.4σ was three times greater than the next highest peak. The solution showed the enzyme in the same position and orientation as in the wild-type form 2 crystals. The program O was used for manual adjustment of the model to fit the electron density, which was alternated with automated refinement using CNS (*23*, *24*). Automated water picking was performed with CNS and confirmed by visual inspection of $2F_o - F_c$ electron density maps calculated without solvent or substrates present in the phasing model. For the model submitted to the database, refinement was completed with conjugate gradient refinement of atomic positions and restrained individual *B*-factors. An alternative model was used just to check the nature of bound solvent and ions. The *B*-factors of these atoms were reset to their average, and then their occupancies were refined to estimate the number of electrons in each bound ion/molecule to help in their identification. The deduced atom types were used in the final refinement, but otherwise the alternative occupancy-refined model did not contribute to the final model.

Continuum Electrostatics. The program Delphi 3.0 (*25*) was used to determine the electrostatic potential at the chloride site in the C271A crystal structure. The linear Poisson−Boltzmann equation was solved by finite difference methods with the chloride ion removed from the model. The ADP, Mg^{2+}, nitrate, and arginine of the transition state analogue complex were explicitly included, as were crystallographic waters, but hydrogens were incorporated implicitly in a united atom approximation. The dielectric was 4 for the solute, 80 outside the solvent excluded surface, calculated with a probe radius of 1.5 Å. An ionic strength of 0.15 was used at 300 K with a Stern layer (radius of 2.0 Å). Calculations were not sensitive to grid spacing, values of 0.8−1.5 Å being tested. For the p*K* calculations, the program MEAD (*26*) was used with similar parameters to determine electrostatic potential, intrinsic p*K*, and electrostatic interaction energies in both the transition state analogue complex and the substrate-free structure of wild-type arginine kinase. The program *xmcti* (*27*) was used to determine the fraction of each active site titratable group that is protonated/deprotonated, considering the possible charge states of neighboring titratable groups. Atomic charges and radii were assigned using the AMBER94 parameter set (*28*), but other commonly used parameter sets led to only minor changes in p*K* (±0.2). Hydrogen atoms were added to crystallgraphic models prior to electrostatic calculations using the Leap module of AMBER6 (*29*).

Homology Modeling. Arginine kinase was a relatively tractable example of homology modeling because closely related structures could be used as starting points, and experimental structures of mutants (*20*) were available to evaluate the computational procedures. The starting point for homology modeling was the 1.2 Å resolution transition state analogue structure refined to an R_{cryst} of 12% (*30*). Initial models were constructed using the builder module of InsightII or DeepView/Swiss-PdbViewer (*31*). The side chain of residue 271 was changed to S, N, or D and modeled as the standard rotamer with least steric conflicts. Energy minimization was performed using the AMBER94 force field as a part of the Sander module of the AMBER6 software package (*29*). Simulations included the entire protein (residues 2−357), substrates arginine and ADP, nitrate mimicking the transition state γ-phosphoryl, and 501 crystallographically observed water molecules. It also included a shell of 3774 explicitly simulated water molecules (that had not been observed crystallographically) forming a truncated octahedron surrounding the protein and crystallographically observed solvent atoms by at least 5 Å. Protons and the explicit solvent shell were added using the Leap module of AMBER6 (*29*).

Energy minimizations were performed with a truncated octahedral periodic box, with a harmonic restraint of 1 kcal/(mol·Å) on solute atoms. Minimizations proceeded until the derivative of the energy function decreased below 0.05 kcal/(mol·Å) over about 5000 cycles. Then each model was subjected to simulated annealing followed by slow cooling. The annealing schedule increased the temperature from 1 to 800 K over the first 1000 cycles (1 ps). The temperature was maintained at 800 K from 5 to 10 ps; then the system was slowly cooled from 800 to 0 K over the next 5−15 ps. During simulated annealing, atoms beyond a 15 Å radius of residue 271 were restrained to their starting locations with a harmonic restraint of 50 kcal/mol, while most atoms within the 15 Å radius were restrained with a weak 0.2 kcal/(mol·Å) force constant. The strong restraints far from the active site allowed conformational searches using aggressive annealing strategies without disrupting the overall structure. Weak restraints close to a site of perturbation are commonly applied, as here, to suppress gratuitous changes. Active site residues with atoms that were moved in any experimental mutant structure and those closest to Cys_{271} were free to move

Table 1: Steady-State Enzyme Kinetic Parameters Determined in the Reverse Reaction Direction (ATP Formation) at pH 7 and with Chloride Concentrations of (A) 1 mM or (B) 60 mM

	wild type	C271S	C271A	C271N	C271D
(A) 1 mM chloride					
K_M(phosphoarginine)	0.45 ± 0.06	7.6± 0.4	1.6 ± 0.1	1.2 ± 0.2	4.4 ± 1.3
K_M(ADP)	0.04 ± 0.01	0.2 ± 0.2	0.30 ± 0.09	0.17 ± 0.01	0.10 ± 0.04
α	0.27 ± 0.04	1.0 ± 0.2	1.1 ± 0.2	1.4 ± 0.4	0.8 ± 0.5
k_{cat}	104 ± 24	0.07 ± 0.02	0.08 ± 0.03	0.022 ± 0.002	1.2 ± 0.4
% wild-type k_{cat}[a]	72	0.05	0.06	0.02	0.82
(B) 60 mM chloride					
K_M(phosphoarginine)	0.30 ± 0.09	0.8 ± 0.3	5.4± 1.9	1.30 ± 0.08	7.5 ± 3.6
K_M(ADP)	0.04 ± 0.02	0.17 ± 0.07	0.17 ± 0.04	0.31 ± 0.03	0.21 ± 0.04
α	0.40 ± 0.01	0.95 ± 0.2	0.5 ± 0.15	1.7 ± 0.5	1.2 ± 0.6
k_{cat}	145 ± 14	0.3 ± 0.2	1.5 ± 0.4	0.042 ± 0.003	1.2 ± 0.2
% wild-type k_{cat}[a]	100	0.22	1.02	0.03	0.83

[a] Relative to wild type in 60 mM chloride.

without any harmonic restraints. Unrestrained residues included 270−272, 224−226, and 313−316 from all three of the four active site loops that contact the substrate arginine guanidinium.

The ability of the protocols to predict structures was tested with control simulations, the results of which could be compared to known experimental structures. These were increasingly ambitious but started with the wild-type structure to verify that the procedures did not cause the structure to diverge from the experimental one. The root mean square deviation (rmsd) for the unrestrained atoms near Cys_{271} was 0.68 Å, elevated due to apparent flexibility in the side chains of Glu_{314} and His_{315}. Prediction of the C271A structure from the wild type was a realistic test for the prediction of other Cys_{271} conservative mutations. The simulated model successfully predicted the largest changes, modest movements of the substrate arginine and movement of His_{315}. The rmsd for the unrestrained atoms close to residue 271 was 0.43 Å (compared to the experimental structure). Prediction of the E314D structure (*20*) was a test of the method's ability to predict larger perturbations: about 1 Å in the backbone of Asp_{314} and His_{315} and larger in the side chains. Predicted models replicated the backbone shift within 0.5 Å and correctly identified a 180° rotation of His_{315} about χ_2, leading to an interaction with the carboxylate of the substrate arginine. The predicted and experimental conformations of the mutated side chain at residue 314 show different positions of C_β, but rotations about χ_1 and χ_2 torsion angles result in a single carboxylate oxygen interacting with substrate arginine, as observed crystallographically. Thus, even in challenging cases, where there is some discrepancy in atomic positions, the procedures correctly predict the principal atomic interactions.

RESULTS

Expression and Purification. Expression of active site cysteine mutants C271A, C271S, C271N, and C271D resulted in yields similar to that of wild type AK with approximately 30 mg of highly pure protein resulting from a 1 L bacterial culture (*19*). These mutants all yielded normally folded enzyme with measurable activity. Several other mutants yielded only lower quantities (<6 mg) of mostly or completely misfolded enzyme, often as a white precipitate. C271G was inactive and, despite testing many refolding protocols, consistently gave an S100 size-exclusion chromatographic profile characteristic of misfolded arginine kinase. C271T yielded low levels of activity and an S100 profile indicating both folded and misfolded enzyme similar to wild-type arginine kinase. C271M and C271Y yielded no measurable activity. Full kinetic analysis was continued with the C271A, C271S, C271N, and C271D mutants that could be folded normally, while mutants C271G, C271T, C271M, and C271Y were not pursued further.

Kinetic Evaluation of Cys271 Mutants. All Cys_{271} mutants displayed dramatically reduced k_{cat} (turnover) values ranging from 0.02% to 1.0% of wild type (Table 1). Increased chloride concentration from 1 to 60 mM elicited 20- and 4-fold increases in the k_{cat} of C271A and C271S mutants, respectively (Table 1). In fact, the highest activity observed among mutants was C271A in 60 mM chloride. The C271D mutant showed approximately 30-fold higher activity than the isosteric C271N (Table 1). C271D was slightly less active than C271A, but its activity (k_{cat} = 0.8% wild type) was independent of chloride concentration. In the absence of a negatively charged side chain at residue 271, or chloride in the assay mixture, serine, alanine, and asparagine mutants displayed only 0.02−0.06% of wild-type activity.

Steady-state kinetic measurements of substrate binding were made for wild type and mutants in solutions containing 1 or 60 mM chloride, using the reverse direction of the reaction toward ATP production (Table 1). Kinetic constants for the wild-type AK were consistent with prior studies (*20*). All kinetic plots for wild-type arginine kinase and mutants were consistent with the random order bi-bi mechanism (data not shown). The turnover rates (above) and the kinetic binding constants (below) were determined for each construct using at least three independent determinations. Here, the Cleland notation is used with K_{ia} denoting an "initial" (binary) kinetic dissociation constant between a single substrate and free enzyme (denoted by other authors sometimes as K_s or K_d). K_M is the (ternary) kinetic dissociation constant for the Michaelis complex with both substrates. The synergy coefficient α is the ratio of K_M/K_{ia}. A value of α <1 indicates that the binding of the second substrate is enhanced by the presence of the first (*32*).

The pattern of change in phosphoarginine and ADP binding constants in Cys_{271} mutants is complex, with significant increases being observed in K_{ia} and K_M for C271D and chloride-dependent changes in K_{ia} and K_M for C271A and C271S mutants (Table 1). C271A showed a significant increase in the observed K_{ia} and K_M for phosphoarginine upon addition of 60 mM chloride to the reaction mixture, while

C271S showed an opposite effect as K_{ia} and K_M for phosophoarginine decreased from significantly elevated levels in 1 mM chloride to near wild-type values in 60 mM chloride. Comparison of C271D steady-state binding constants with those determined for isosteric C271N showed that K_{ia} and K_M for phosphoarginine were increased in C271D, while C271N values were much closer to wild type.

Several overall trends in the kinetic parameters are obvious. The kinetic dissociation constants of phosphoarginine are more greatly affected by mutation at Cys_{271} than those of the nucleotide. This is expected due to the proximity of Cys_{271} to the guanidino substrate. For the nucleotide substrate, it is the K_M that is affected more than K_{ia}, consistent with an indirect interaction between Cys_{271} and the nucleotide substrate mediated by binding of the other (phosphagen) substrate. With the exception of C271S, the effects of Cys_{271} mutation and added chloride upon kinetic measures of phosphoarginine binding can be explained in terms of electrostatic repulsion between phosphoarginine and the variable side chain of residue 271 or a chloride ion. In the thiolate form of cysteine (wild type) or the carboxylate in C271D, a negatively charged side chain may repel phosphoarginine. In C271A, where extra space is available, a chloride replacing the thiolate sulfur at high concentration may also impair phosphoarginine binding. All mutants exhibited less substrate synergy than wild-type arginine kinase, with α values closer to unity. Lost synergy results from larger changes in K_M than K_{ia} for mutants relative to wild type. In contrast to significantly unfavorable synergy observed in active site cysteine mutants of Mi_b-CK, only the C271N mutant displayed any unfavorable substrate synergy with α near 2. However, in other ways the kinetic effects of cysteine mutations in arginine kinase are similar to those observed for similar mutations in Mi_b-CK (*13*), so there is no reason to believe that the mechanisms are fundamentally different.

Structure Determination of the C271A Transition State Analogue Complex. Extensive efforts to crystallize active site cysteine mutants resulted in diffraction quality crystals of C271A only. Clusters of C271A crystals appeared after 4 days, and single crystals grew to about $0.25 \times 0.25 \times 0.10$ mm^3 in 2−4 weeks. Thus they were smaller than wild type but nearly isomorphous in unit cell parameters with wild-type transition state complex form 2 crystals (*19*). The structure, solved by molecular replacement, includes residues 2−357, one ADP molecule, one nitrate ion, one magnesium ion, one chloride ion, and 313 water molecules. Model statistics include $R_{free} = 23.1\%$ and $R = 20.6\%$. Cross-validated Luzzati analysis gives an estimated coordinate error of 0.34 Å (Table 2).

Identification of Chloride in the Active Site. After placement of 313 water molecules and individual *B*-factor refinement, the average *B*-factor for solvent atoms was 52 $Å^2$, but one water molecule had an exceptionally low *B*-factor of 7 $Å^2$. *B*-factors for all solvent atoms were set equal to the average for solvent atoms, and the occupancy values of these atoms were refined. The water molecule of interest refined to an occupancy value of 3, clearly above the occupancy of all other solvent water molecules. The electrostatic potential was calculated for this "water" site by numerically solving the linear Poisson−Boltzmann equation using the program Delphi (*25*). The site coincided with a positive peak in the electrostatic potential. On the basis of the high occupancy, positive electrostatic potential, and the presence of 100 mM $MgCl_2$ in crystallization setups, this water molecule was replaced by a chloride ion in the final model.

Table 2: Crystallographic and Refinement Statistics

arginine kinase	C271A
crystal form	$P2_12_12_1$
a (Å)	64.9
b (Å)	71.3
c (Å)	80.0
temperature (K)	100
resolution (Å)	2.3 (2.38−2.30)
completeness (%)	93.2 (92.2)
redundancy[a]	3.3
R_{merge}[b] (%)	7.5 (19.9%)
R_{cryst}[c] (%)	20.9 (32.8)
R_{free}[d] (%)[e]	23.6 (33.5)
cross-validated Luzzati error (Å)[e]	0.34 (10−2.3)

[a] Average number of observations of each reflection. [b] $R_{merge} = \sum|I_h - \langle I_h\rangle|/\sum|I_h|$, where $\langle I_h\rangle$ is the average intensity of symmetry-equivalent observations. [c] $R_{cryst} = \sum|F_o - F_c|/\sum|F_o|$, the conventional crystallographic refinement *R*-factor. [d] R_{free} is the cross-validated *R*-factor, calculated the same way, except with a random set (3%) of reflections omitted from the structure determination and refinement. [e] See ref *46*.

Position of Chloride. Chloride ions act as strong hydrogen bond acceptors and are usually coordinated by three or four ligands in trigonal or pyramidal configurations, although, like water, there is not great directional specificity to the coordination (*33*). In the structure of C271A four polar ligands are observed: the $N_{\eta 1}$ of the substrate arginine, a water molecule, and the backbone nitrogen and the hydroxyl of threonine 273 (Figure 1b). Among the ligands, the presumptive hydrogen-bonding interactions between chloride and protein atoms are similar to those seen in small organic molecules (*34*) and in atomic resolution protein crystal structures (*35*, *36*). One methyl and two methylene groups also contact chloride at distances between 3.15 and 3.6 Å.

Comparison between Transition State Structures of C271A and Wild-Type Arginine Kinase. The overall fold of C271A is nearly identical to the wild-type AK transition state structure, with a rmsd of 0.36 Å over all 356 C_α atoms. Comparison between wild type and C271A shows five stretches of four or more residues with statistically significant differences between the two models. In the amino-terminal domain, residues 2−9, 34−38, and 89−92 are displaced approximately 0.5 Å from wild-type positions. These changes are minor, distant from the active site, and therefore not likely to be important to catalysis. The largest changes are in the carboxyl-terminal domain between residues 291 and 300. Residues 294−300 are α-helical as they are in the wild-type transition state structure but not in the substrate-free structure. However, in C271A the helix is translated about 2 Å toward the active site, resulting in new interactions for Arg_{294}: a hydrogen bond to the backbone oxygen of Thr_{316} and, through a water, to His_{315} (Figure 3). Glu_{314} and His_{315} interact with the substrate arginine, the side chain of His_{315} moving 0.8 Å to form a hydrogen bond with the substrate arginine N_ϵ (Figure 3). Neighboring loop residues 315−321 have backbone displacements of approximately 0.5 Å. With the kinetic binding constants suggesting weaker binding, movement of loops away from substrate arginine might have been expected, but in fact, the loop comes closer to substrate arginine (Figure 3). Other flexible active site loops are

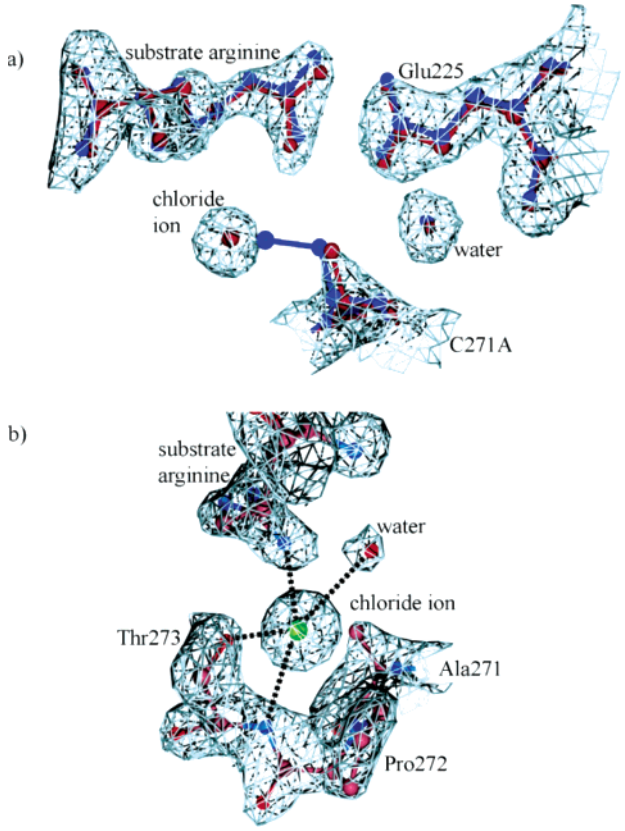

FIGURE 1: (a) Structures of C271A (red) and wild type (blue) overlaid on the C271A experimental electron density, phased with the final refined model. The $2F_o - F_c$ electron density map at 2.3 Å resolution, contoured at 1.8σ, clearly shows a lack of density for sulfur of residue 271 and a strong peak of electron density modeled as chloride. The map also shows that the small changes in the position of substrate arginine resulting from automated refinement against diffraction amplitudes may not be experimentally significant. (b) Coordination of a single chloride ion in the active site of C271A arginine kinase. The chloride ion is coordinated by the nonreactive N_η of substrate arginine (3.4 Å), the hydroxyl oxygen of T273 (2.8 Å), the backbone nitrogen of T273 (3.3 Å), and a bound water molecule (3.4 Å).

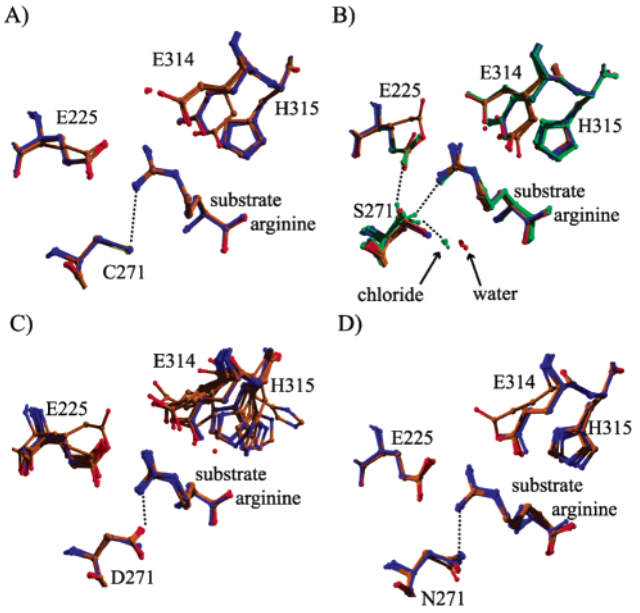

FIGURE 2: Ensembles of simulated arginine kinase structures showing the changed interactions near the site of various Cys_{271} mutations. Differences between ensemble members arise when different random initial trajectories for the molecular dynamics simulations converge upon structures with very similar calculated potential energies. In all panels the experimental wild-type transition state structure is shown in blue, and distances are given in angstroms (Å). (A) A simulation of the wild-type arginine kinase was performed as one of the controls, and it shows little deviation from the experimental structure except for the loop holding Glu_{314} and His_{315} that appears to be more flexible than other active site loops. (B) Simulated models of C271S with and without an active site chloride ion. Models simulated with a chloride ion in the active site are shown in green. Several rotamers are observed for the serine side chain, all of similar total energy and without van der Waals overlap. (C) C271N models indicate that the added size of an asparagine can be accommodated without great perturbation to the rest of the active site. The amide oxygen is closer (~3.3 Å) to the substrate guanidinium than the amide nitrogen, but it is unable to achieve an ideal hydrogen-bonding configuration. (D) C271D models show a potential salt bridge/hydrogen-bonding interaction between the carboxylate of Asp_{271} and the substrate arginine N_η (~2.7 Å).

unchanged relative to the wild-type transition state structure. Overall, the locations of the greatest changes are similar to the E314D mutant (*20*).

Active Site. The positions of ADP and nitrate in the C271A structure do not differ from wild type significantly (with reference to cross-validated Luzzati estimates of coordinate error). The changes in the substrate arginine are slightly greater. The guanidino N_η atoms move 0.4−0.5 Å toward the space vacated by the sulfur in C271A. This shift of the guanidinium relative to the nitrate and MgADP results in modest perturbation of substrate alignment in the transition state analogue complex. Although the guanidinium displacement is nominally greater than the average coordinate error (0.34 Å), the refined C271A structure fits the 2.3 Å $2F_o - F_c$ electron density map only marginally better than wild type (Figure 1a), giving little support for the significance of this structural difference. The difference map, calculated with F_o-(wild type) − F_o(C271A) coefficients, should be most sensitive to conformational differences. The highest positive peak corresponds to the loss of Cys_{271}'s sulfur, and the largest negative peak corresponds to the insertion of the neighboring chloride in C271A. No difference electron density was observed near the reactive nitrogen $N_{\eta 2}$. In summary, the diffraction data show clearly that the C271A mutation has introduced a new chloride binding site within 2 Å of the sulfur that is now missing, but the impact upon the rest of the active site is minimal, barely detectable at 2.3 Å resolution.

C271S,N,D Homology Models. Homology models of C271S, C271N, and C271D were constructed to help to rationalize the kinetic effects of Cys_{271} substitutions in mutants that were not amenable to crystallization. C271S was modeled without and with an active site chloride, initially positioned as in the C271A crystal structure, but allowed to move unrestrained during energy minimization and simulated annealing.

In homology models, the side chains of Asp_{314} and His_{315} showed a variety of conformations of nearly equal energy, suggesting that a variety of conformations are possible in this loop (Figure 2). There are several experimental indications that this region is intrinsically less stable than other parts of the active site. This loop was completely disordered in all phosphagen kinase structures determined in the absence of bound substrates but is clearly observed in transition state analogue complexes of both AK and CK as well as a binary

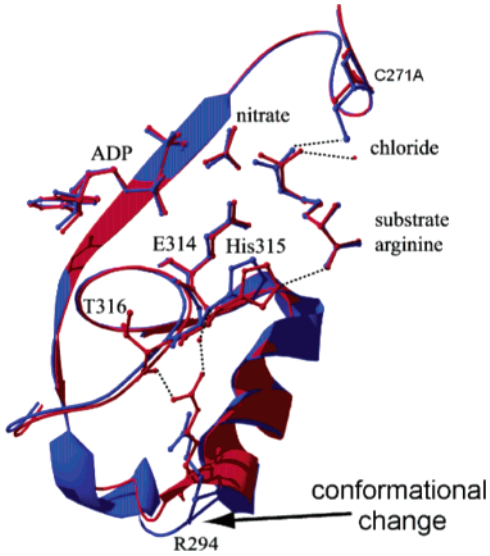

FIGURE 3: Selected atoms from the wild-type arginine kinase transition state analogue complex (blue) and C271A (red) showing the largest conformational change observed in the mutant and how this change can be traced back to the active site of the enzyme. The connection between Arg_{294} to Thr_{316} and His_{315} is shortened by one coordinating water molecule in the mutant relative to wild type. A result is a new hydrogen bond between His_{315} and a carboxylate oxygen of substrate arginine in C271A.

complex of creatine kinase with MgADP (*8*, *37*). In arginine kinase, the loop structure is modestly affected by mutation at residue 225, another active site residue with which it makes no direct interaction (*20*). Thus, it appears that variability between members of a molecular dynamics ensemble (each member started with a different random trajectory) is at least a qualitative indicator of the stability of active site residues.

Side chain conformational variability was also seen at the serine in the C271S mutant. In the initial model, several rotamers could be built without steric overlap, so the rotamer homologous to the native cysteine was chosen. Simulated annealing of a chloride-free model with different random trajectories resulted in three side chain positions with nearly equal energy. The slightly reduced size and charge neutrality of the serine appear to give greater freedom to the serine than the native cysteine. One conformation was similar to the wild-type cysteine, but with the γ-hydroxyl moved slightly closer to the hydroxyl of T273 and the substrate guanidinium. Two other rotamers offer alternative hydrogen bonds for the hydroxyl, either with a carboxylate oxygen of Glu_{225} and the guanidinium of substrate arginine or away from the Glu_{225} carboxylate and toward a simulated water molecule. In simulations with a chloride ion, the ion remained within 1 Å of its position in the experimental C271A structure, between 3.5 and 4 Å from the positively charged guanidinium of substrate arginine (Figure 1b). Simulations of C271S with chloride resulted in different side chain orientations than simulations without chloride. Three distinct side chain conformations were found with interactions of its γ-hydroxyl to both the chloride (3 Å) and the nonreactive N_η of substrate arginine (3−3.1 Å). A fourth rotamer was found within 2.7 Å of a carboxylate oxygen of Glu_{225}, nearly 4 Å from the N_η of substrate arginine and 5 Å from the chloride ion. By constrast, there was little ensemble variation in either the C271D or C271N mutants. In C271D one carboxylate oxygen interacted with the nonreactive N_η of substrate arginine and a bound water molecule, and the other carboxylate oxygen formed hydrogen-bonding interactions with the hydroxyl oxygen and backbone nitrogen of Thr_{273}, as well as the backbone nitrogen of Pro_{272}, all at distances between 2.6 and 3.0 Å. The carboxylate of Glu_{225} was also displaced from its wild-type position in one of the C271D ensemble models, but mostly it remained in its wild-type conformation. In the C271N models the side chain amide oxygen makes the closest interactions with the guanidinium (3.2−3.4 Å) from the nonreactive N_η but forms a more optimal hydrogen-bonding interaction with the hydroxyl of Thr_{273} at 2.8 Å. The amide nitrogen of the substituted asparagine hydrogen bonds to the backbone carbonyl of Ile_{67} and a water molecule. In summary, the simulations show that all of the conservative mutations expressed experimentally can be accommodated without major perturbations to the active site. More detailed analysis will follow in the Discussion.

DISCUSSION

Enzyme kinetic analyses of arginine kinase and creatine kinase have demonstrated similar millisecond time scales and substrate binding affinities for the two enzymes (*3*, *38*). Here, mutations of the active site cysteine yielded results similar to those for Mi_b-CK(*13*) and human muscle CK (*14*). Catalysis was markedly reduced, and kinetic dissociation constants were slightly increased for the phosphagen substrate, indicating weaker binding. The most active arginine kinase cysteine mutants are slightly less active than creatine kinase. No direct comparison was possible to the 10% active Mi_b-CK C278G mutant due to misfolding of the arginine kinase C271G mutant. However, the arginine kinase mutant C271A has activity (1%) that is nearly as high as this and the HMCK C282S mutant (4%) (*14*).

Taken together, the kinetic results from homologous family members present a strong argument that the cysteine is not absolutely essential for catalysis. The overall similarity in the kinetics of cysteine mutants also makes a strong case that while detailed differences may exist, the cysteine acts in a fundamentally similar role in each of these homologous enzymes. That said, the availability of a high-resolution mutant structure (C271A) for arginine kinase now eliminates the popularly held belief that the primary role of the cysteine is in execution of large substrate-induced conformational changes (*13*). The C271A structure is in the transition state form and, apart from very local changes, is in a wild-type configuration. Clearly, some other rationalization of the importance of the cysteine is needed. Past considerations of the role were based on categorization of mutants as active or inactive, but partial activity may be key to understanding the cysteine. The case is made below that several active site amino acids enhance the enzymatic rate through the catalytic chemistry or alignment of substrates. The leading role of the cysteine may be catalytic, even if it is only responsible for part of the catalytic effect.

The kinetics and structure reported here give strong and mutually consistent support to the proposal that the cysteine functions as a thiolate ion (*13*, *14*, *39*). As with creatine kinase (*13*), chloride can partially rescue the activity of Cys_{271} mutants. The C271A structure shows that the chloride binds close to the position of the negatively charged sulfur in wild

type, substituting, in part, for its role. The rescue effect is greatest for the C271A mutation where the chloride gets closest to the native sulfur position. Simulation of the C271S structure shows that, consistent with the chloride dependence of its kinetics, a chloride can be accommodated, but it would require a change in the serine side chain conformation from that of the wild-type cysteine. Simulation of the C271N structure predicts that a chloride would not be bound in the immediate vicinity of the guanidinium, consistent with the kinetics showing little effect of chloride, less than observed in Mi_bCK (*13*). As might be expected, chloride provides no further help to the C271D mutant that is already negatively charged. The predicted C271D structure indicates that the wild-type thiolate−guanidinium interaction is replaced by a carboxylate−guanidinium salt bridge (2.7 Å), although the carboxylate oxygen position differs slightly from that of the sulfur.

The C271A mutant shows that the effect of the chloride is mediated through catalysis. In fact, substrate binding is actually less favorable with higher K_M and K_{ia} for phosphoarginine as chloride concentration is increased. The earlier studies with Mi_bCK found unfavorable impact of chloride upon phosphocreatine binding in most cysteine mutants (*13*). Here, it is seen only for the alanine mutation that allows chloride binding close to the native thiolate position and not for the asparagine and aspartate mutants (Table 1). This, and the higher dissociation constants for C271D, can be rationalized in terms of electrostatic repulsion between phosphoarginine and a negatively charged active site. Direct electrostatic effects cannot explain the behavior of C271S. One of the several predicted rotamers moves the hydroxyl away from the guanidino nitrogen to hydrogen bond to Glu_{225}, perturbing the p*K* of Glu_{225} and likely diminishing the interaction between Glu_{225} and substrate arginine.

The loss of synergistic substrate binding upon mutation or chemical modification of creatine kinase had been cited as supporting the previously proposed role of the cysteine in a substrate-induced conformational change (*10*, *13*). Here, with arginine kinase, the effects upon synergy are less pronounced. Our C271A mutant crystal structure shows that the cysteine is not required for the substrate-induced conformational change, but there are other ways that synergy could be mediated. With the cysteine in thiolate form (see below), electrostatics is a possibility. Synergy could be impacted by perturbations in the juxtaposed charged substrates, and the neighboring active site residues that provide countercharges, or by other subtle conformational changes local to the active site.

It has been noted previously that the reported p*K* of creatine kinase's active site cysteine is perturbed down from 8.5 to one of the kinetic p*K*s at 5.4 (*14*). Titration of the 240 nm absorption, characteristic of thiol groups, was used to show that the p*K* of the cysteine was low (p*K* 5.6) even in the absence of substrates (*14*). While there are other precedents of active site cysteines with low p*K*, in the phosphagen kinase substrate-free form, there is no basic residue with which the cysteine could form an ion pair, the usual mechanism for p*K* perturbation (*40*−*42*). The cysteine's p*K* is perturbed by one unit by the hydrogen bond with Thr_{273} (*7*) or a homologous serine in creatine kinase (*14*), but the means with which a larger p*K* perturbation is made remains a mystery. Here, application of the Poisson−Boltzmann equation (*43*) to the refined transition state analogue arginine kinase structure (*18*) gives a calculated p*K* of 6.1. This excellent agreement with the kinetic p*K* (*14*, *44*) demonstrates that the electrostatic environment in the substrate-bound state is sufficient to account for the low p*K*. By contrast, calculation using the substrate-free structure (*16*) yields only a slightly lowered p*K* of 7.5. Comparisons with experimental p*K*s of many other proteins has demonstrated that the accuracy of such calculations is usually better than 1 p*K* unit (*45*). There is a caveat that the present calculations omit an active site loop that has not been ordered in any of the substrate-free structures (*16*), but the loop is remote from Cys_{271} and unlikely to have great impact. The current calculation makes intuitive sense, suggesting that the low p*K* thiolate form is stabilized with the formation of an ion pair as the guanidino substrate binds. Thus, substrate binding and the rationalization of kinetic dissociation constants are complicated by the likely loss of the thiolate proton as the substrate binds.

Questions about cysteine's protonation state in the substrate-free form relate to matters of substrate binding. However, the larger impact of the Cys_{271} mutations is upon catalytic rate. Many arguments now implicate the thiolate form in catalysis: (1) kinetic p*K*s were determined from homologous creatine kinase mutants (*14*); (2) of mutations at the active site cysteine in several homologous enzymes, negatively charged aspartate substitutions are among those partially active (ref *13* and this work); (3) for mutational substitution of small amino acids for the cysteine, chloride is able to partially rescue activity in several of these enzymes (ref *13* and this work); (4) in arginine kinase, the chloride has been shown to bind to mutants at a site close to the native location of the negatively charged sulfur and to form analogous interactions with the substrate arginine (this work); (5) electrostatic calculations using the atomic structure indicate that when substrates are bound, Cys_{271} of arginine kinase has a p*K* of 6.1 and is predominantly deprotonated (this work).

How the thiolate contributes to catalytic enhancement without being absolutely essential is open to speculation. One possibility is that the negative charge and proton affinity (basic character) of the thiolate would draw positive charge to the unreactive N_η, perturbing the resonance of the guanidinium. The effect would be to increase the double-bonded nature between the C_ζ and the unreactive N_η while decreasing it between the C_ζ and the reactive N_η. For the forward reaction (phosphoarginine forming), this would enhance the nucleophilicity of the reactive N_η whose lone pair attacks the γ-phosphorus of ATP. For the reverse reaction (ATP forming), minimization of any double-bonding character of the reactive N_η would enhance the leaving group properties of the arginine and assist the phosphoryl transfer to ADP. Such a role could involve proton transfer from guanidinium to cysteine, and later back again, or the effect might fall short of formal transfer, requiring only that the proton be drawn toward the thiolate.

The potential role of a conserved active site cysteine has been debated for over 40 years. Here, with the addition of structure, a role of the active site cysteine in mediating induced-fit conformational changes is ruled out, implicating the cysteine in catalysis again. However, these and other studies of active site residues (*20*) indicate that the enzyme

embodies several strategies simultaneously for enhancing the catalytic rate and that there are several residues that contribute to the overall rate enhancement, none of which are absolutely required for the reaction to proceed at a measurable rate.

ACKNOWLEDGMENT

We gratefully acknowledge Rani Dhanarajan and the Molecular Cloning Facility and T. Somasundaram of the X-ray Facility at Florida State University for help. We also thank Heather Carlson and Kristen Meagher of the University of Michigan for supplying AMBER94 force-field modifications for ADP. Data were collected at the Southeast Regional Collaborative Access Team (SER-CAT) 22-ID (or 22-BM) beamline at the Advanced Photon Source, Argonne National Laboratory. Use of the Advanced Photon Source was supported by the Department of Energy, Office of Science, Office of Basic Energy Sciences, under Contract W-31-109-Eng-38.

REFERENCES

1. Kenyon, G. L., and Reed, G. H. (1983) Creatine Kinase: Structure−activity Relationships, *Adv. Enzymol. 54*, 367−426.
2. Ellington, W. R. (2001) Evolution and Physiological Roles of Phosphagen Systems, *Annu. Rev. Physiol. 63*, 289−325.
3. Blethen, S. L. (1972) Kinetic Properties of the Arginine Kinase Isoenzymes of *Limulus polyphemus*, *Arch. Biochem. Biophys. 149*, 244−251.
4. Hansen, D. E., and Knowles, J. R. (1981) The Stereochemical Course of the Reaction Catalyzed by Creatine Kinase, *J. Biol. Chem. 256*, 5967−5969.
5. Morrison, J. F. (1973) in *The Enzymes* (Boyer, P. D., Ed.) pp 457−486, Academic Press, New York.
6. Virden, R., and Watts, D. C. (1966) The Role of Thiol Groups in the Structure and Mechanism of Action of Arginine Kinase, *Biochem. J. 99*, 162−172.
7. Zhou, G., Somasundaram, T., Blanc, E., Parthasarathy, G., Ellington, W. R., and Chapman, M. S. (1998) Transition state structure of arginine kinase: Implications for catalysis of bimolecular reactions, *Proc. Natl. Acad. Sci. U.S.A. 95*, 8449−8454.
8. Lahiri, S. D., Wang, P. F., Babbitt, P. C., McLeish, M. J., Kenyon, G. L., and Allen, K. N. (2002) The 2.1 A Structure of *Torpedo californica* Creatine Kinase Complexed with the ADP-Mg^{2+}-NO_3^--Creatine Transition-State Analogue Complex, *Biochemistry 41*, 13861−13867.
9. Watts, D. C., and Rabin, B. R. (1962) A Study of the "Reactive" Sulphydryl Groups of Adenosine 5′-triphosphate-Creatine Phosphotransferase, *Biochem. J. 85*, 507−516.
10. Maggio, E. T., and Kenyon, G. L. (1977) Properties of a CH3-blocked creatine kinase with altered catalytic activity. Kinetic consequences of the presence of the blocking group, *J. Biol. Chem. 252*, 1202−1207.
11. Wu, H., Yao, Q.-Z., and Tsou, C.-L. (1989) Creatine kinase is modified by 2-chloromercuri-4-nitrophenol at the active site thiols with complete inactivation, *Biochim. Biophys. Acta 997*, 78−82.
12. Hornemann, T., Rutishauser, D., and Wallimann, T. (2000) Why is creatine kinase a dimer? Evidence for cooperativity between the two subunits, *Biochim. Biophys. Acta 1480*, 365−373.
13. Furter, R., Furter-Graves, E. M., and Wallimann, T. (1993) Creatine Kinase: The Reactive Cysteine Is Required for Synergism But Is Nonessential for Catalysis, *Biochemistry 32*, 7022−7029.
14. Wang, P. F., McLeish, M. J., Kneen, M. M., Lee, G., and Kenyon, G. L. (2001) An unusually low p*K*(a) for Cys282 in the active site of human muscle creatine kinase, *Biochemistry 40*, 11698−11705.
15. Lin, L., Perrymann, M. B., Friedman, D., Roberts, R., and Ma, T. S. (1994) Determination of the Catalytic Site of Creatine Kinase by Site-directed Mutagenesis, *Biochim. Biophys. Acta 1206*, 97−104.
16. Yousef, M. S., Clark, S. A., Pruett, P. K., Somasundaram, T., Ellington, W. R., and Chapman, M. S. (2003) Induced fit in guanidino kinases-comparison of substrate-free and transition state analogue structures of arginine kinase, *Protein Sci. 12*, 103−111.
17. Fritz-Wolf, K., Schnyder, T., Wallimann, T., and Kabsch, W. (1996) Structure of Mitochondrial Creatine Kinase, *Nature 381*, 341−345.
18. Yousef, M. S., Fabiola, F., Gattis, J. L., Somasundaram, T., and Chapman, M. S. (2002) Refinement of the arginine kinase transition-state analogue complex at 1.2 A resolution: mechanistic insights, *Acta Crystallogr., Sect. D: Biol. Crystallogr. 58*, 2009−2017.
19. Zhou, G., Parthasarathy, G., Somasundaram, T., Ables, A., Roy, L., Strong, S. J., Ellington, W. R., and Chapman, M. S. (1997) Expression, Purification from Inclusion Bodies, and Crystal Characterization of Transition State Analog Complex of Arginine Kinase: a Model for Studying Phosphagen Kinases, *Protein Sci. 6*, 444−449.
20. Pruett, P. S., Azzi, A., Clark, S. A., Yousef, M., Gattis, J. L., Somasundaram, T., Ellington, W. R., and Chapman, M. S. (2003) The putative catalytic bases have, at most, an accessory role in the mechanism of arginine kinase, *J. Biol. Chem. 29*, 26952−26957.
21. Segel, I. H. (1975) in *Enzyme Kinetics—Behaviour and Analysis of Rapid Equilibrium and Steady-State Enzyme Systems*, Wiley, New York.
22. Otwinowski, Z., and Minor, W. (2001) in *International Tables for Crystallography. Crystallography of Biological Molecules* (Rossmann, M. G., and Arnold, E., Eds.) pp 226−235, International Union of Crystallography, Dortrecht.
23. Brünger, A. T., Adams, P. D., Clore, G. M., Gros, P., Gross-Kunstleve, R. W., Jiang, J.-S., Kurzewski, J., Nilges, M., Pannu, N. S., Read, R. J., Rice, L. M., Simonson, T., and Warren, G. L. (1998) Crystallography and NMR system: A new software system for macromolecular structure determination, *Acta Crystallogr. D54*, 905−921.
24. Kleywegt, G. J., and Jones, A. T. (1996) Efficient Rebuilding of Protein Structures, *Acta Crystallogr. D52*, 829−832.
25. Rocchia, W., Alexov, E., and Honig, B. (2001) Extending the Applicability of the Nonlinear Poisson−Boltzmann Equation: Multiple Dielectric Constants and Multivalent Ions, *J. Phys. Chem. B 105*, 6507−6514.
26. Bashford, D. (1997) in *Lecture Notes in Computer Science: Scientific Computing in Object-Oriented Parallel Environments* (Ishikawa, Y., Oldehoeft, R. R., Reynders, J. V. W., and Tholburn, M., Eds.) pp 233−240, Springer, Berlin.
27. Beroza, P., and Case, D. A. (1998) Calculations of proton-binding thermodynamics in proteins, *Methods Enzymol. 295*, 170−189.
28. Bayly, C. I., Cieplak, P., Cornell, W., and Kollman, P. A. (1993) A well-behaved electrostatic potential based method using charge restraints for deriving atomic charges: the RESP model, *J. Phys. Chem. 97*, 10269−10280.
29. Case, D. A., Pearlman, D. A., Caldwell, J. W., Cheatham, T. E., III, Ross, W. S., Simmerling, C. L., Darden, T. A., Merz, K. M., Stanton, R. V., Vincent, J. J., Crowley, M., Ferguson, D. M., Radmer, R. J., Seibel, G., Singh, U. C., Weiner, P. K., Caldwell, J., and Kollman, P. A. (1999) Amber 5.0, University of California, San Francisco.
30. Yousef, M. S., Fabiola, F., Gattis, J., Somasundaram, T., and Chapman, M. S. (2002) Refinement of Arginine Kinase Transition State Analogue Complex at 1.2 Å resolution; mechanistic insights, *Acta Crystallogr., Sect. D: Biol. Crystallogr. 58*, 2009−2017.
31. Guex, N., and Peitsch, M. C. (1997) SWISS-MODEL and the Swiss-PdbViewer: an environment for comparative protein modeling, *Electrophoresis 18*, 2714−2723.
32. Segel, I. H. (1975) *Enzyme Kinetics—Behaviour and Analysis of Rapid Equilibrium and Steady-State Enzyme Systems*, Wiley Classics Edition, 1993 ed., Wiley, New York.
33. Jeffrey, G. A., and Saenger, W. (1991) *Hydrogen Bonding in Biological Structures*, Springer-Verlag, Berlin.
34. Steiner, T., Schreurs, A. M. M., Kanters, J. A., and Kroons, J. (1998) Water molecules hydrogen bonding to aromatic acceptors of amino acids: the structure of Tyr-Tyr-Phe dihydrate and a crystallographic database study on peptides, *Acta Crystallogr. 54*, 25−31.
35. Ridder, I. S., Rozeboom, H. J., and Dijkstra, B. W. (1999) Haloalkane dehalogenase from *Xanthobacter autotrophicus* GJ10 refined at 1.15 Å resolution, *Acta Crystallogr. D55*, 1273−1290.
36. Backstrom, S., Wolf-Watz, M., Grundstrom, C., Hard, T., Grundstrom, T., and Sauer, U. H. (2002) The RUNX1 Runt domain at

1.25 Å resolution: a structural switch and specifically bound chloride ions modulate DNA binding, *J. Mol. Biol. 322*, 259−272.
37. Zhou, G., Wang, J., Blanc, E., and Chapman, M. S. (1998) Determination of the Relative Precision of Atoms in a Macromolecular Structure, *Acta Crystallogr. D54*, 391−399.
38. Kuby, S. A., Noda, L., and Lardy, H. A. (1954) Adenosinetriphosphate-Creatine Transphosphorylase III. Kinetic Studies, *J. Biol. Chem. 210*, 65−82.
39. Watts, D. C. (1973) in *The Enzymes* (Boyer, P. D., Ed.) pp 383−455, Academic Press, New York.
40. Polgar, L., and Halasz, P. (1973) On the reactivity of the thiol group of thiolsubtilisin, *Eur. J. Biochem. 39*, 421−429.
41. Gladysheva, T., Liu, J., and Rosen, B. P. (1996) His-8 lowers the pK_a of the essential Cys-12 residue of the ArsC arsenate reductase of plasmid R773, *J. Biol. Chem. 271*, 33256−33260.
42. Lo Bello, M., Parker, M. W., Desideri, A., Polticelli, F., Falconi, M., Del Boccio, G., Pennelli, A., Federici, G., and Ricci, G. (1993) Peculiar spectroscopic and kinetic properties of Cys-47 in human placental glutathione transferase. Evidence for an atypical thiolate ion pair near the active site, *J. Biol. Chem. 268*, 19033−19038.
43. Yang, A. S., Gunner, M. R., Sampogna, R., Sharp, K., and Honig, B. (1993) On the calculation of pK_as in proteins, *Proteins 15*, 252−265.
44. Cook, P. F., Kenyon, G. L., and Cleland, W. W. (1981) Use of pH Studies to Elucidate the Catalytic Mechanism of Rabbit Muscle Creatine Kinase, *Biochemistry 20*, 1204−1210.
45. Antosiewicz, J., McCammon, J. A., and Gilson, M. K. (1994) Prediction of pH-dependent properties of proteins, *J. Mol. Biol. 238*, 415−436.
46. Brünger, A. T. (1997) The Free *R* Value: A More Objective Statistic for Crystallography, *Methods Enzymol. 277*, 366−396.

BI049793I